Chapter 5

INTERFACE

Interface is a very general term used in various fields of science and technology to denote the location where two entities meet. The term in composites refers to a bounding surface between the reinforcement and matrix across which there is a discontinuity in chemical composition, elastic modulus, coefficient of thermal expansion, and/or thermodynamic properties such as chemical potential. The interface (fiber/matrix or particle/matrix) is very important in all kinds of composites. This is because in most composites, the interfacial area per unit volume is very large. Also, in most metal matrix composite systems, the reinforcement and the matrix will not be in thermodynamic equilibrium, i.e., a thermodynamic driving force will be present for an interfacial reaction that will reduce the energy of the system. All these items make the interface have a very important influence on the properties of the composite.

Instead of a bidimensional boundary, generally, we have an interfacial zone with finite thickness, possibly consisting of multiple layers. The multilayer boundary zone will be in equilibrium at the high temperature at which the components were originally brought together. At any other temperature, a complex stress field exists in the boundary zone because of mismatch in coefficient of thermal expansion of the various layers. These stresses will be proportional to the difference in the elastic moduli of the components, difference in the coefficients of thermal expansion, and of course the temperature difference between the equilibrium (or initial) temperature and final temperature. Thermodynamically speaking, the phases in the boundary zone will tend to change such that the free energy of the system is minimized. This may involve generation of dislocations, grain boundary migration, crack nucleation and/or propagation. An ideal interface in a metal matrix composite should promote wetting and bond the reinforcement and the matrix to a desirable degree. The interface should protect the ceramic

reinforcement and allow load transfer from the soft metallic matrix to the strong reinforcement.

Besides composition, we also need to take into account other parameters that characterize the interfacial zone such as: Geometry and dimensions; microstructure and morphology; and mechanical, physical, chemical, and thermal characteristics of the different phases present in the interfacial zone.

The components of a composite system are chosen on the basis of their mechanical and physical characteristics in isolation. When one puts together two components to make a composite, the system will rarely be in thermodynamic equilibrium. More often than not, a driving force will be present for some kind of interfacial reaction(s) between the two components leading to a state of thermodynamic equilibrium. Of course, thermodynamic information such as phase diagrams can help predict the final equilibrium state of the composite. Data regarding reaction kinetics, for example, diffusivities of one constituent in another can provide information about the rate at which the system will tend to equilibrium. In the absence of thermodynamic and kinetic data, experimental studies need to be conducted to determine compatibility of the components.

In this chapter, we first describe some important concepts related to interfaces in metal matrix composites. Types of bonding in MMCs are provided with examples from various systems, followed by a description of some tests to determine the mechanical properties of interfaces.

5.1 CRYSTALLOGRAPHIC NATURE OF THE INTERFACE

In crystallographic terms, one can describe an interface between two crystalline phases as coherent, semi-coherent, or incoherent. A coherent interface implies one-to-one correspondence between lattice planes on the two sides of the interface. The lattice constants of any two phases are not likely to be the same. Thus, in order to provide continuity of lattice planes across an interface, i.e., a coherent interface, there will be some coherency strains associated with the interface because of straining of the lattice planes in the two phases. Commonly, such coherent interfaces are observed between some precipitates and the metallic matrix where the mismatch in the lattice parameter of the two phases is quite small. For example in the Al-Li system, Al_3Li precipitate is coherent with the aluminum matrix. An incoherent interface, on the other hand, consists of such severe atomic disorder that no matching of lattice planes occurs across the boundary, i.e., no continuity of lattice planes is maintained across the interface. Thus, an

incoherent boundary or interface will have no coherency strains but the energy associated with the interfacial boundary increases because of severe atomic disorder. A situation that is intermediate between coherent and incoherent can exist, i.e., we can have a semi-coherent interface. A semi-coherent interface has some lattice mismatch between the phases which can be accommodated by the introduction of dislocations at the interface. Crystallographically, most of the interfaces that one encounters in fiber, whisker, or particle reinforced metal matrix composites are incoherent and high energy interfaces. Accordingly, they can act as efficient vacancy sinks, and provide rapid diffusion paths, segregation sites, sites of heterogeneous precipitation, as well as sites for precipitate-free zones. Among the possible exceptions to this are eutectic composites and XD-type particulate composites, in which the interfaces can be semi-coherent.

5.2 WETTABILITY

Wettability is defined as the ability of a liquid to spread on a solid surface. Figure 5.1 shows two conditions of a liquid drop resting on a solid substrate. There are three specific energy (energy per unit area) terms: γ_{SV}, the energy of the solid/vapor interface; γ_{LS}, the energy of the liquid/solid interface; and γ_{LV}, the energy of the liquid/vapor interface. It should be mentioned that the term surface tension is also used to denote surface energy, although rigorously speaking, surface energy is a more appropriate term for solids. When we put a liquid drop on a solid substrate, we replace a portion of the solid/vapor interface by a liquid/solid and a liquid/vapor interface. Thermodynamically, spreading of the liquid will occur if this results in a decrease in the free energy of the system, i.e.:

$$\gamma_{SL} + \gamma_{LV} < \gamma_{SV}$$

Figure 5.1 defines these terms. An important parameter with respect to wettability is the contact angle, θ, which is a measure of wettability for a system. From the equilibrium of forces in the horizontal direction, we can write:

$$\gamma_{SL} + \gamma_{LV} \cos\theta = \gamma_{SV}$$
$$\theta = \cos^{-1}(\gamma_{SV} - \gamma_{SL})/\gamma_{LV}$$

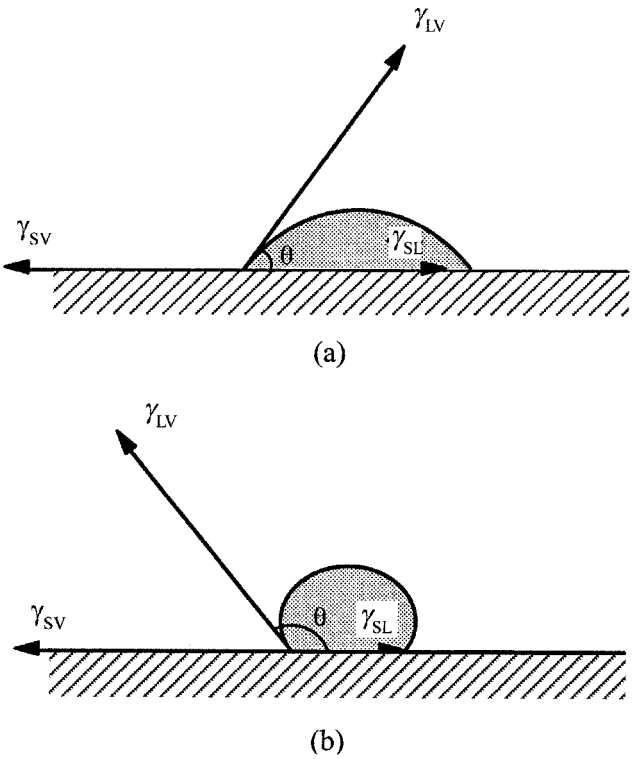

Fig. 5.1 Contact angle, θ, a measure of wettability for a system is defined by interaction among three surface energies: Solid-liquid surface energy, γ_{SL}, solid-vapor surface energy, γ_{SV}, and liquid-vapor surface energy, γ_{LV}.

From this equation, we see that for $\theta = 0^\circ$, we have perfect wetting, while for $\theta = 180^\circ$, we have no wetting. For $0^\circ < \theta < 180^\circ$, there will be partial wetting. It should be pointed out that the contact angle for a given system can vary with temperature, stoichiometry, hold time, interfacial reactions, presence of any adsorbed gases, roughness and geometry of the substrate, etc.

It is worth emphasizing that wettability only describes the extent of intimate contact between a liquid and a solid. It does not necessarily mean a strong bond at the interface. One can have excellent wettability but only a weak physical, low energy bond. A low contact angle, implying good wettability, is a necessary but not sufficient condition for strong bonding. Wettability of the ceramic reinforcement by the molten metal is very important for liquid state processing of MMCs. One can modify the contact angle by changing the composition of the liquid matrix, which changes the value of its surface

energy. The effect of roughness of the solid substrate can be evaluated in terms of a ratio, r, defined as:

$$r = \frac{\text{true surface area}}{\text{mean plane surface area}}$$

In general, if $\theta < 90^{\circ}$, wettability is enhanced by roughness while if $\theta > 90^{\circ}$, wettability is reduced by roughness.

5.3 TYPES OF BONDING

There are two important types of bonding at an interface in a metal matrix composite:

- Mechanical bonding
- Chemical bonding

A brief description of mechanical and chemical bonding is given below with examples from various MMC systems.

5.3.1 Mechanical Bonding

Most fibers have a characteristic surface roughness or texture resulting from the fabrication process (techniques for measuring fiber roughness are shown in the inset.) This in turn imparts a roughness to the interface when the fibers are incorporated in a matrix to make a composite. Mechanical keying of the matrix into the hills and valleys of the surface of the reinforcement (due to roughness) is an important but generally neglected aspect of the interface in all composites. It turns out that interface roughness-induced mechanical bonding is quite important in all kinds of composites. Surface roughness can contribute to bonding only if the liquid matrix wets the reinforcement surface. If the liquid matrix (polymer, metal, or ceramic) is unable to penetrate the asperities on the fiber surface, then the matrix will leave interfacial voids on solidification. In a mechanical bond, the degree of interfacial roughness is a very important parameter, which, in turn, is controlled by the fiber surface roughness. In polymer matrix composites (PMCs) and metal matrix composites (MMCs), one would like to have mechanical bonding in addition to chemical bonding. In ceramic matrix composites (CMCs), one would like to have mechanical bonding rather than chemical bonding. In fiber reinforced composites mechanical bonding will be effective mostly in the longitudinal or fiber direction. Transverse to the fiber, it will provide only a minor effect.

Techniques for Measuring Roughness

Most fibers have surface markings or *striations* that originate from the edges of the surface of the spinneret or the edges of a die, in the case of wire drawing. Thus, the origin of surface roughness lies in processing. Such roughness is characterized by rather close and irregular changes in surface height, resulting in peaks and valleys about an imaginary mean surface line. A whole range of techniques is available for measuring surface roughness. In a mechanical profilometer, a diamond stylus is run over the surface and the up and down movement of the stylus is recorded. Atomic Force Microscopy (AFM) can offer a greater spatial resolution than any of the conventional techniques. The best mechanical profilometer can resolve variations in surface heights down to 0.1 μm, while the AFM can resolve heights as small as 1 nm. Scanning tunneling microscope (STM) can be used to characterize an electrically conducting surface. STM detects changes in the quantum-mechanical tunneling current of electrons between the surface and an electrode (W or Pt) as the electrode scans the surface. The magnitude of tunneling current decreases with distance between the electrode and the surface. This can be used to provide information about the topography of the surface. AFM can characterize most any material, including an electrically insulating material such as a glass or a ceramic. Commonly a silicon or silicon nitride tip is used at the end of a microcantilevered arm. Atomic forces (van der Waals or electrostatic) between the tip and the surface deflect the arm, with the deflection falling off with distance from the surface. The deflection is higher for peaks and lower for valleys. A laser beam from a laser diode is reflected off the back of the cantilever with an optical-lever detection system. Conventionally, a stylus-based profilometer provides height information in one direction. In this regard, AFM can be regarded as a high magnification profilometer that has a superior vertical and lateral resolution. AFM is controlled by a microprocessor that provides a variety of computer-based topographical images of the surface. For example, gray scale (and/or color images) can be obtained, in which x and y data form the horizontal and vertical axes while the z-data are used to give the gray scale. The gray scale is a linear scale in which the brightness of a point is in proportion to its height. A brighter point corresponds to a higher height while a darker point corresponds to a lower height on the surface. One can then draw a line across the gray scale image and display the surface topographical profile corresponding to the line. The figure on the next page shows an AFM picture of the surface of a Nicalon fiber and the roughness profile corresponding to the line between the arrows in the AFM picture.

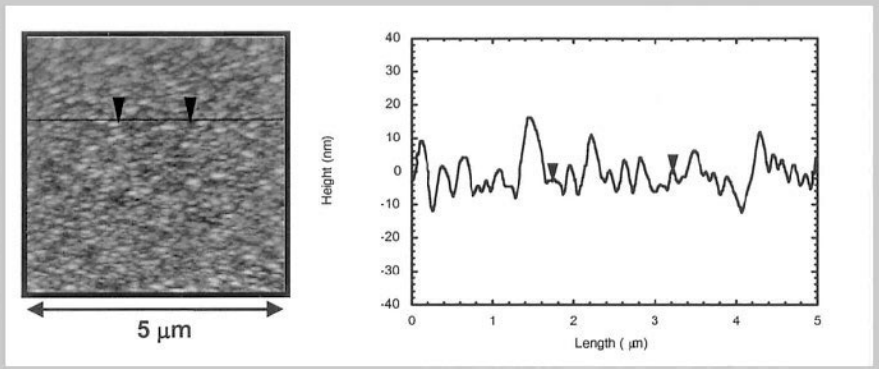

Another possibility is a three-dimensional representation of the surface wherein the height is indicated by superimposing the gray scale along the perpendicular axis and rotating the display to a convenient viewing angle. A three-dimensional picture of the surface of Nicalon fiber is shown in figure below (Chawla et al., 1995). It is possible to further enhance the three-dimensional aspect by adding a computer-generated light source to cast shadows. This is called illumination mode, not shown here.

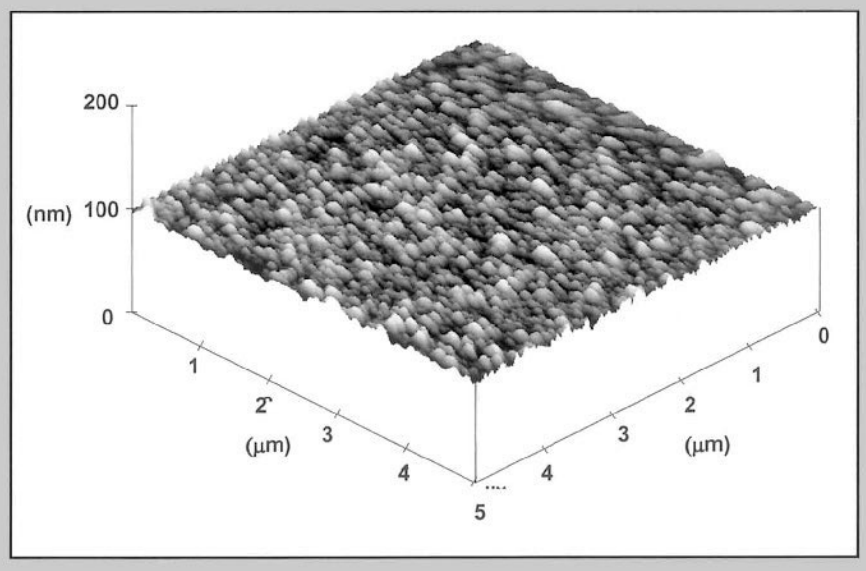

Mechanical keying between two surfaces can lead to bonding between them and can be quite important in metal matrix composites. An ideal, smooth interface is only an idealization. Interfaces in real composites are invariably rough, which allows for interlocking. The degree of interfacial roughness can be controlled to some extent, but there is always some mechanical bonding present. Consider the situation of an MMC made of a ceramic reinforcement and a metallic matrix. Metals generally have a higher coefficient of thermal expansion than ceramics. Thus, the metallic matrix in the composite will shrink radially more than the ceramic fiber on cooling from a high temperature. This will lead to mechanical gripping of the fiber by the matrix even in the absence of any chemical bonding. The matrix penetrating the crevices on the fiber surface, by liquid flow or high temperature diffusion, can also lead to some mechanical bonding. The radial gripping stress, σ_r, can be related to the interfacial shear strength, τ_i, by the following expression:

$$\tau_i = \mu\sigma_r$$

where μ is the coefficient of friction, generally, between 0.1 and 0.6. In general, a mechanical bond is a low energy bond vis-à-vis a chemical bond. Examples of mechanical bonding include alumina fibers in a variety of metals, e.g., Al_2O_3 fiber in aluminum. Mechanical bonding with carbon fibers is improved by chemically treating the surface with nitric acid. The oxidation of the fiber surface results in increased specific surface area of the fibers.

We cite two examples showing the importance of mechanical gripping effects in MMCs. Hill et al. (1969) confirmed this experimentally for tungsten filaments in an aluminum matrix while Chawla and Metzger (1978) observed mechanical gripping effects at Al_2O_3/Al interfaces. Hill et al. (1969) etched tungsten wires along a portion of their length to produce a rough interface. In the first work, tungsten filaments were incorporated into an aluminum matrix by liquid metal infiltration technique in vacuum. They evaluated three interface conditions by longitudinal tensile tests of composites. In the case of a smooth interface, a chemical bond formed between the aluminum matrix and tungsten fiber, which resulted in a high strength composite. In the case of a smooth fiber surface with a graphite layer, the graphite barrier layer prevented the reaction from taking place, that is, there was no chemical bonding, and because the interface was smooth (little or no roughness), there was also very little mechanical bonding. The resultant strength of the composite was, therefore, very low. In the third case, they etched the tungsten filaments and applied a graphite

layer. In this case, there was no reaction bonding, but there was a mechanical keying effect because of the rough surface produced by etching. The result was that the mechanical bonding restored the strength of the composite to the level achieved with chemical reaction at the interface. Chawla and Metzger (1978) compared the load transfer from aluminum to alumina as a function of interfacial roughness. They used a polished aluminum surface and roughened aluminum surface produced by etch-pitting. Alumina was formed by electrolytically anodizing the aluminum. When this composite was loaded in tension, the crack appeared in the alumina perpendicular to the loading direction. Figure 5.2 shows these results in the form of linear crack density (number of cracks per unit length) in alumina as a function of strain in the alumina/aluminum composite for different degrees of interface roughness. Solid circles represent the polished substrate or smooth interface while filled squares represent steep sided pits (10^6 pits/cm^2) or rough interface. Cracks in the alumina film first appeared at about the same strain. Initially the crack density rose at about the same rate for the rough and smooth interfaces. For a smooth interface, however, the crack density remained constant above 8% strain in the matrix while for a rough interface, the crack density continued to increase beyond this value, i.e., in the case of a rough interface the load transfer from aluminum to alumina continued to higher strain values than in the case of a smooth interface. Thus, high degree of mechanical bonding at the rough interface was responsible for more efficient load transfer from the soft aluminum matrix to hard alumina. Similar mechanical bonding effects due to interface roughness have been observed in babbitt (Sn with small amounts of Cu and Sb)-bronze composites (Liaw et al., 1990).

5.3.2 Chemical Bonding

Ceramic/metal interfaces in metal matrix composites are generally formed at high temperatures. Diffusion and chemical reaction kinetics are faster at elevated temperatures. Knowledge of the chemical reaction products and, if possible, their properties are needed. It is therefore imperative to understand the thermodynamics and kinetics of reactions such that processing can be controlled and optimum properties obtained.

Chemical bonding in MMCs involves atomic transport by diffusion. Thus, chemical bonding includes solid solution and/or chemical compound formation at the interface. It may lead to the formation of an interfacial zone containing a solid solution and/or a reinforcement/matrix interfacial reaction zone.

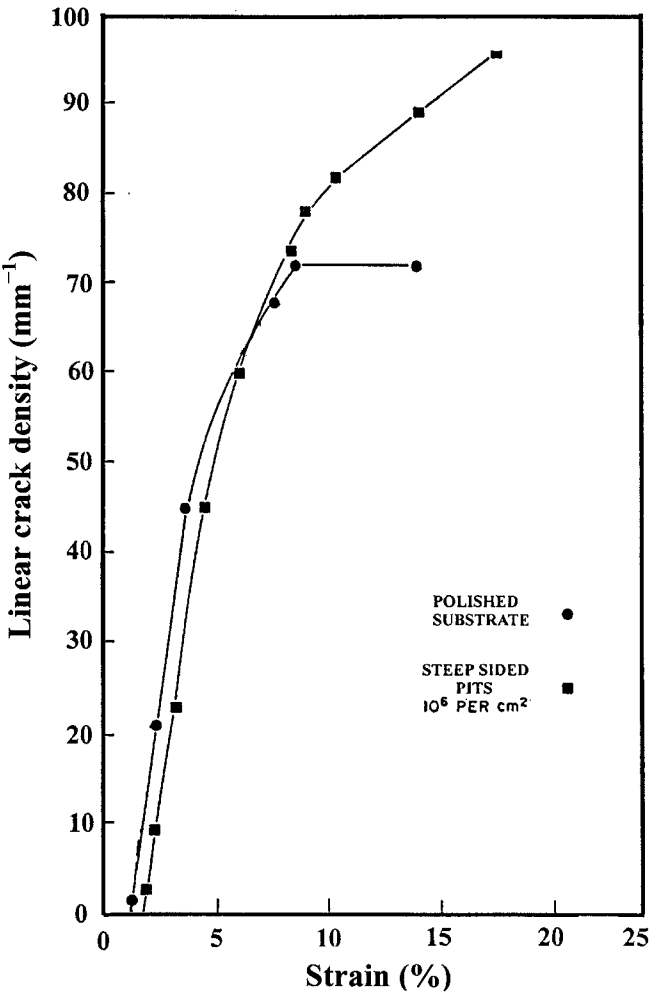

Fig. 5.2 Load transfer from aluminum to alumina as a function of interfacial roughness (after Chawla and Metzger, 1978). For a smooth interface, the crack density remained constant above 8% strain in the matrix while for a rough interface, the crack density continued to increase beyond this value, i.e., the load transfer from aluminum to alumina continued to higher strain values in the case of a rough interface.

For diffusion controlled growth in an infinite diffusion couple with a planar interface, we have the following important relationship:

$$x^2 \approx Dt$$

where x is the thickness of the reaction zone, D is the diffusivity, and t is time. The diffusivity, D, depends on the temperature in an exponential manner:

$$D = D_o \exp(-\Delta Q / kT)$$

where D_o is a pre-exponential constant, ΔQ is the activation energy for the rate controlling process, k is the Boltzmann's constant, and T is the temperature in kelvin. For a composite containing small diameter cylindrical fibers, the assumption of an infinite diffusion couple is not valid, i.e., the diffusion distances are quite small. However, to a first approximation, we can write:

$$x^2 \approx Bt$$

where B is a pseudo-diffusivity constant and has the dimensions of diffusivity, i.e., m^2s^{-1}. One may use this approximate relationship for composites where the thickness of the reaction zone is small compared to the interfiber spacing. Under these conditions, one can use an Arrhenius type relationship:

$$B = A \exp(-\Delta Q / kT)$$

where A is a pre-exponential constant. A plot of ln B vs. 1/T can then be used to obtain the activation energy, ΔQ, for a fiber/matrix reaction in a given temperature range. The dependence of the reaction zone thickness on the square root of time indicates the operation of volumetric diffusion. Figure 5.3 shows in a schematic manner the effect of temperature on the reaction zone thickness vs. $\sqrt{}$time. With increasing temperature, the slope of the line increases.

As we said above, most metal matrix composite systems are nonequilibrium systems in the thermodynamic sense; that is, a chemical potential gradient exists across the fiber/matrix interface. This means that given favorable kinetic conditions, which in practice means a high enough temperature or long enough time, diffusion and/or chemical reactions occur between the components. Prolonged contact between liquid metal and reinforcement can lead to a significant chemical reaction, which may adversely affect the

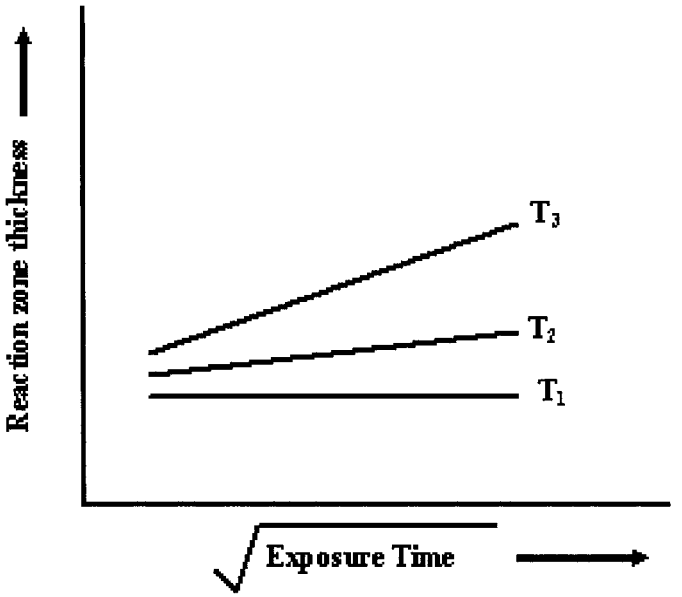

Fig. 5.3 Schematic representation of thickness of reaction zone between fiber and matrix as a function of square root of exposure time for three different temperatures, $T_3 > T_2 > T_1$.

behavior of the composite. For example, molten aluminum can react with carbon fiber to form Al_4C_3 and Si per the following reaction:

$$4Al + 3SiC \longleftrightarrow Al_4C_3 + 3Si$$

This reaction, as indicated by the two arrows, can go leftward or rightward. When it goes rightward, it injects silicon in the molten aluminum, which can have important consequences. Change of matrix alloy composition is one. Addition of silicon in aluminum also results in lowering of the melting point of the alloy; in fact it will result in a mushy range. Kinetics, i.e., time and temperature will control the Si level required to prevent the reaction. This reaction can be prevented from going rightward by using high levels of Si in the matrix, say ~ 10% Si. It is for this reason that only high silicon aluminum alloys are suitable for SiC particles for making composites by casting route. Al_2O_3 is stable in pure molten aluminum. It does, however, react with magnesium, a common alloying element in aluminum. The following reactions can occur between Mg and Al_2O_3:

$$3Mg + Al_2O_3 \longleftrightarrow 3MgO + 2Al$$

$$3Mg + 4Al_2O_3 \longleftrightarrow 3MgAl_2O_4 + 2Al$$

In alumina reinforced composites with a high level of Mg in the matrix, MgO is expected to form at the interface, while spinel forms at low levels of Mg (Pfeifer et al., 1990).

Figure 5.4 shows a transmission electron microscopy (TEM) micrograph of the reaction zone between alumina fiber and magnesium matrix made by liquid metal infiltration. The interface layer(s) formed generally have characteristics different from those of either one of the components. At times some controlled amount of reaction at the interface may be desirable for obtaining strong bonding between the fiber and the matrix; too thick an interaction zone, of course, adversely affects the composite properties.

The importance of matrix alloy composition cannot be over-emphasized. For example, in pure Mg matrix, SiC particle would be stable and no reaction is observed at the interface. In Mg alloys containing Al and Si as the main alloying elements, interfacial reaction can occur between Al and SiC as described above. Such a reaction will form the undesirable Al_4C_3 and inject Si into the matrix, which can react with Mg to form Mg_2Si. Another important composite system involves SCS-6 type silicon carbide fiber and a titanium alloy (Ti-6Al-4V) matrix. Interfacial reaction products in this case include TiC and Ti_xSi_y (Gabryel and McLeod, 1991).

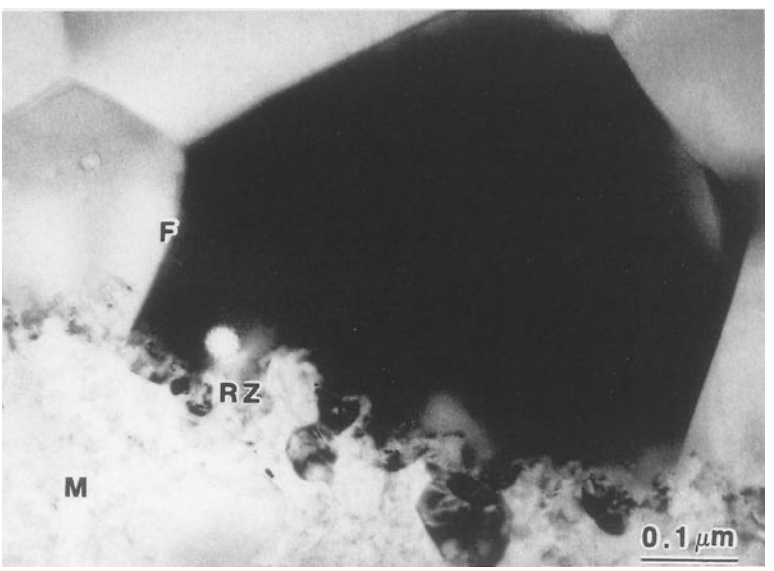

Fig. 5.4 Bright field (BF) transmission electron micrograph showing interface in a continuous fiber (F) α-Al_2O_3/Mg alloy (ZE41A) matrix (M). RZ indicates the interfacial reaction zone.

We provide a summary of interfacial reaction products in some important metal matrix composites in Table 5.1. It is important to have an understanding of the structure and properties of the reaction products that form in a given system because they will be the key in determining the final properties of the composite. For example, in carbon fiber reinforced aluminum processed at around 700°C, Al_4C_3 forms. It is also very sensitive to ambient moisture. It would be very desirable to avoid formation of such brittle phases at the interface because they lead to catastrophic failure of the composite.

5.3.3 Interactions at the Interface due to Thermal Mismatch

Thermal stresses arise in composite materials because of the mismatch between the coefficients of thermal expansion of the components making up the composite. Mismatch in elastic constants of the components exacerbates the problem. In a fiber reinforced composite, if the matrix thermal expansion coefficient is higher than that of the fiber, then on cooling from high temperature radial compression will result, i.e., the matrix will grip the fiber. Such radial gripping of the fiber by the matrix will increase the

Table 5.1: Interfacial reaction products in some important MMCs

Reinforcement	**Matrix**	**Reaction product(s)**
SiC	Ti alloy Aℓ alloy	TiC, Ti_5Si_3 $Aℓ_4C_3$
$Aℓ_2O_3$	Mg alloy	MgO, $MgAℓ_2O_4$ (spinel)
$Aℓ_20_3$	Aℓ alloy	None
B	Aℓ alloy	$AℓB_2$
ZrO_2	Aℓ alloy	$ZrAℓ_3$
C	Aℓ alloy	$Aℓ_4C_3$
C	Cu	None
W	Cu	None
NbTi Nb_3Sn	Cu	None
Various Oxides	Ag	None

strength of the interface. This increases the tendency toward brittleness in the composite. This will make phenomena such as fiber debonding and pullout, desirable for enhanced toughness, difficult to operate.

Quite frequently, the very process of fabrication of a composite can involve interfacial interactions that can cause changes in the constituent properties and/or interface structure. For example, if the fabrication process involves cooling from high temperatures to ambient temperature, then the difference in the expansion coefficients of the two components can give rise to thermal stresses of such a magnitude that the softer component (generally the matrix) will deform plastically. Chawla and Metzger (1972) studied a tungsten reinforced single crystal copper matrix (non-reacting components). They observed that liquid copper infiltration of tungsten fibers at about 1100°C, followed by cooling to room temperature, resulted in a dislocation density in the copper matrix that was much higher in the vicinity of the interface than away from the interface. The high dislocation density in the matrix near the interface resulted from the plastic deformation of the matrix caused by high thermal stresses near the interface. Other researchers observed similar results in other systems such as SiC whiskers in an aluminum matrix (Arsenault and Fisher, 1983) and short alumina fibers in aluminum matrix (Dlouhy et al., 1993). If powder metallurgy fabrication techniques are used, the nature of the powder surface will influence the interfacial interactions. For example, an oxide film on the powder surface affects its chemical nature. Topographic characteristics of the components can also affect the degree of atomic contact obtainable between the components. This can result in geometrical irregularities (e.g., asperities and voids) at the interface, which can be source of stress concentrations.

5.4 MEASUREMENT OF INTERFACIAL BOND STRENGTH

Once the matrix and the reinforcement of a composite are chosen, it is the set of characteristics of the interface region that determines the final properties of the composite. In this regard, thorough characterization of the interface region assumes a great deal of importance. A variety of sophisticated techniques are available to mechanical characterization of the interface region. In particular, a quantitative measure of the strength of the interfacial bond between the matrix and reinforcement is of great importance. We describe below some of the important techniques to measure interfacial bond strength.

5.4.1 Bend Tests

Bend tests are easy to perform but they do not give a true measure of the interfacial strength. We describe some variants of bend tests below.

Transverse Bend Test

A three-point bend test configuration with fibers aligned perpendicular to the specimen length is called a transverse bend test. There are two possible arrangements of fibers, one with fibers parallel to the length of the specimen and the other with fibers transverse to the length of fibers. Under either one of these configurations, fracture will occur on the outermost surface of the specimen which is under maximum tensile stress. This will put the fiber/matrix interface under tension, which gives us a measure of tensile strength of the fiber/matrix interface. The transverse strength is given by:

$$\sigma = \frac{3PS}{2bh^2} \tag{5.1}$$

where P is the applied load, S is the load span, b is the specimen width, and h is the specimen height.

Longitudinal Bend Test or Short Beam Shear Test

This test is also known as the *I*nter*L*aminar *S*hear *S*trength (ILSS) test. In this test, the fibers are aligned parallel to the length of the three-point bend bar. In such a test, the maximum shear stress, τ, occurs at the midplane and is given by:

$$\tau = \frac{3P}{4bh} \tag{5.2}$$

where the symbols have the significance given above.

The maximum tensile stress occurs at the outermost surface and is given by Eq. 5.1. Dividing Eq. 5.2 by Eq. 5.1, we get:

$$\frac{\tau}{\sigma} = \frac{h}{2S} \tag{5.3}$$

Inspection of Eq. (5.3) shows that we can maximize the shear stress by making the load span, S, arbitrarily small. This ensures that the specimen fails predominantly under shear with a crack running along the midplane. The test becomes invalid if the fibers fail in tension before shear induced failure occurs. The test will also be invalid if shear and tensile failure occur simultaneously. It is advisable to make an examination of the fracture surface after the test and make sure that the crack is along the interface and not through the matrix.

5.4.2 Fiber Pullout and Pushout Tests

Single fiber pullout and pushout tests have been devised to measure interfacial characteristics. Such tests give load vs. displacement curves, with the peak load corresponding to fiber/matrix debonding and a frictional load corresponding to the fiber pullout from the matrix. The main simplification that is frequently made in the analysis of such tests involves averaging the load values over the entire interfacial surface area to get the interface debond strength and/or frictional strength. Analytical and finite element analyses show that the shear stress is a maximum close to the fiber end and falls rapidly within a distance of a few fiber diameters. Thus, one would expect the interface debonding to start near the fiber end and progressively propagate along the embedded length. Here we describe the salient features of these tests.

Single Fiber Pullout Tests

Single fiber pullout tests can provide useful information about the interface strength in *model* composite systems. They are not very helpful in the case of commercially available composites. One must also carefully avoid any fiber misalignment and introduction of bending moments. The mechanics of the single fiber pullout test is complicated (see, e.g., Penn and Lee, 1989; Marshall et al., 1992; Kerans and Parthasarthy, 1991). In all the variants of such test, the fiber is pulled out of the matrix in a tensile testing machine and a load vs. displacement record is obtained.

Figure 5.5 shows the experimental setup for such a test. A portion of fiber, length ℓ, is embedded in a matrix. We apply a pulling tensile force, as shown, and measure the stress required to pull the fiber out of the matrix as a function of the embedded fiber length. The stress required to pull the fiber out without breaking it increases with the embedded fiber length, up to a critical length, ℓ_c. This critical fiber length is the length of fiber that is used in load transfer form matrix to fiber. We discuss the concept of critical fiber

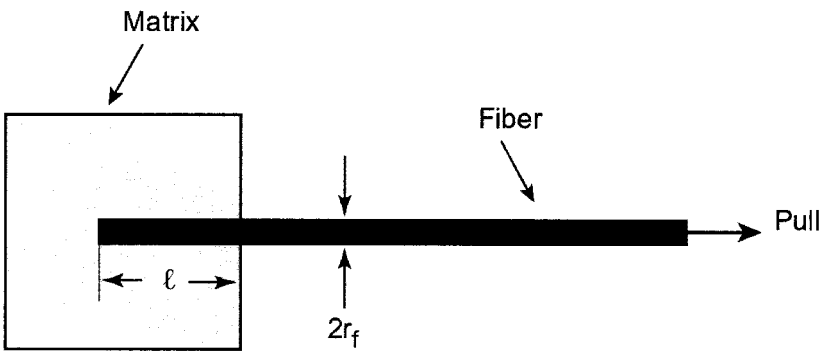

Fig. 5.5 A fiber of radius r embedded in a matrix and being pulled out. The longitudinal tensile force on the fiber generates shear at the fiber/matrix interface.

length in chapter 7. For an embedded fiber length, $\ell > \ell_c$, the fiber will fracture under the action of the tensile stress, σ, acting on the fiber. When we apply a tensile force on the fiber, a shear force at the fiber/matrix interface will result. A simple force balance along the embedded fiber length gives:

$$\sigma\pi r^2 = \tau 2\pi r\ell$$

For $\ell < \ell_c$, the fiber is pulled out and the interfacial shear strength is given by:

$$\tau = \frac{\sigma r}{2\ell}$$

One measures the load, P, required to debond the interface as a function of the embedded fiber length. Then, we can write:

$$P = \tau 2\pi r\ell$$

and the interfacial shear strength, τ, can be calculated from the slope of P vs. ℓ plot. For $\ell > \ell_c$, fiber failure rather than pullout occurs. The interfacial shear strength is a function of the coefficient of friction, μ, and any normal compressive stress at the interface, σ_r, i.e., $\tau_i = \mu\sigma_r$. As mentioned above, a common source of radial compressive stress is the shrinkage of the matrix during cooling from the processing temperature. The most doubtful assumption in this analysis is that the shear stress acting along the fiber/matrix interface is a constant.

The fabrication of the single fiber pullout test sample is often the most difficult part; it entails embedding a part of the single fiber in the matrix. The peak load corresponds to the initial debonding of the interface. This is followed by frictional sliding at the interface, and finally by fiber pullout from the matrix, during which a steady decrease in the load with displacement is observed. The steady decrease in the load is attributed to the decreasing area of the interface as the fiber is pulled out. Thus, the test simulates the fiber pullout that may occur in the actual composite, and more importantly, provides the bond strength and frictional stress values.

The effect of different Poisson contractions of fiber and matrix can lead to a radial tensile stress at the interface. The radial tensile stress will no doubt aid the fiber/matrix debonding process. The effect of Poisson contraction, together with the problem that the imposed shear stress is not constant along the interface, complicates the analysis of fiber pullout test.

Pushout or Indentation Tests

Interfacial frictional sliding is an important characteristic of the fiber/matrix itnerface. Many researchers (for example, Marshall, 1984; Doerner and Nix, 1986; Eldridge and Brindley, 1989; Ferber et al., 1993; Mandell et al., 1986; Mandell et al., 1987; Marshall and Oliver, 1987; Cranmer, 1991; Chawla et al., 2001) have used the technique of pressing an indenter on the cross-section of a fiber in a composite to measure the interfacial bond strength in a fiber/reinforced composite. An instrumented indentation system, the apparatus for which is sometimes called a *nanoindenter*, is available commercially. Such an instrument allows extremely small forces and displacements to be measured. A nanoindenter is essentially a computer-controlled depth-sensing indentation system. Indentation instruments have been in use for hardness measurement since early twentieth century, but "depth sensing" instruments having high resolution became available in the 1980s (Doerner and Nix, 1986; Weihs and Nix, 1991). Very small volumes of material can be studied and a very local characterization of microstructural variations is possible by mechanical means. Indenters with pointed, rounded, and flat tips can be used to displace a fiber aligned perpendicular to the composite surface. By measuring the applied force and the displacement, the interfacial stress can be obtained. One generally loads several fibers in a polished cross section of composite system. Most commercially available nanoindenter instruments are capable of accurately applying very small loads (mN) via a Berkovich pyramidal diamond indenter having the same depth-area ratio as a Vickers diamond tip indenter. A nanoindenter records the total penetration of an indenter into the sample. The

position of the indenter is determined by a sensitive capacitance displacement gage. The capacitance gage can detect displacement changes less than one nm, while the applied force can be detected to less that 1 μN. The indenter can be moved toward the sample or away from the sample by means of a magnetic coil assembly.

In the pushout test, one pushes a fiber out, by means of an indenter, in a thin sample with the fibers aligned perpendicular to the viewing surface. Such a fiber pushout test gives us the frictional shear stress, τ, acting at the fiber/matrix interface. In a valid pushout test, a three-region curve is obtained, see Fig. 5.6. In the first region, the indenter is in the contact with the fiber. Following elastic loading, initial interface debonding takes place. Progressive debonding continues until the interface is fully debonded. This is followed by a horizontal region (region two) which consists of interfacial sliding of the fiber in the matrix. In the third region, the indenter comes in contact with the matrix. From the second region, we can determine the interfacial shear stress. The specimen thickness should be much greater that the fiber diameter for this relationship to be valid. In the horizontal region, the interfacial shear stress is given by:

$$\tau_i = \frac{P}{2\pi rt} \tag{5.4}$$

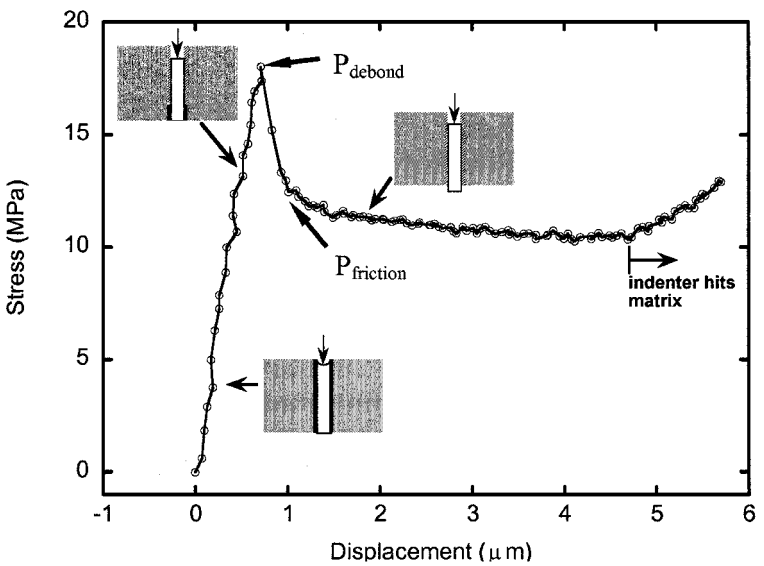

Fig. 5.6 Stress-displacement curve during fiber pushout. After elastic loading, progressive fiber debonding takes place, followed by interfacial sliding (Chawla et al., 2001).

where t is the specimen thickness. In the third region of Fig. 5.6 the indenter comes in contact with the matrix.

If the fiber is strongly bonded to the matrix, the energy at the crack tip at the interface will be high enough to fracture the fiber. In this case, the crack propagates straight through the interface, into the fiber, and the composite fails in a catastrophic manner. If the fiber/matrix interface is tailored, such that bonding between fiber and matrix is weak, a crack propagating normal to the interface will be deflected at the interface, causing it to lose energy. In this manner, debonding and sliding of the fiber with respect to the matrix acts as an energy-absorbing mechanism.

Several important factors control the fiber/matrix behavior, such as thermal residual stresses from processing, that can induce radial clamping stresses and axial stresses from the matrix to the fiber. Thermal mismatch in coefficient of thermal expansion (CTE) between fiber and matrix is responsible for residual stresses in all types of composites (see chapter 6). If the matrix shrinks more than the fiber then a compressive clamping stress will act at the interface

Fiber surface roughness can also contribute significantly to the radial clamping stresses, because the matrix becomes mechanically keyed to the fiber. A roughness induced strain arises because of this mechanical keying, and it can be estimated by the roughness amplitude between fiber and matrix. To relieve radial clamping stresses from CTE mismatch as well as from fiber roughness, a compliant fiber coating can be applied to the fiber. The effect of interfacial clamping stress, temperature, and environment on the debonding and sliding of the pushed fibers was examined by Eldridge and Ebihara (1994). They studied interfacial characteristics in the system SCS-6/Ti-24Al-11Nb (at.%), from ambient temperature to 1100°C. The fiber debond stress and frictional sliding stress decreased continuously at temperatures higher than 300°C, Fig. 5.7. The decrease in interfacial shear strength was attributed to relief of the residual compressive stresses on the fiber, and oxidation of the carbon coating at higher temperatures. Figure 5.8 shows the pushed out fiber at low and high temperatures, showing a relatively rough and smooth surface, respectively.

Eldridge and Ebihara (1994) also showed that the pushout characteristics were a function of environment. They postulated that the sensitivity of the degree of interfacial sliding to the environment can be attributed to the well-documented (Savage, 1948; Lancaster and Pritchard, 1981) to the lubricative properties of graphite, which exists on the outer shell of the

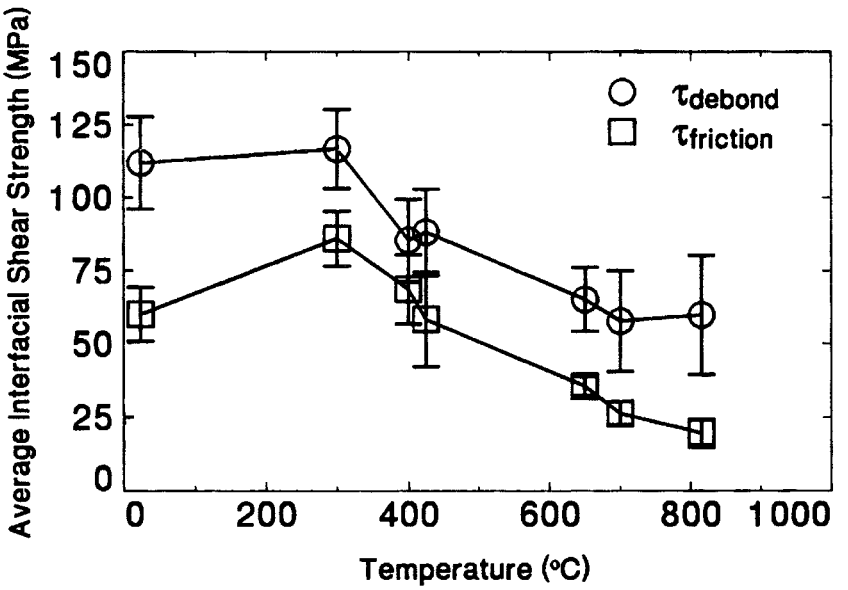

Fig. 5.7 Effect of temperature on fiber debond stress and frictional sliding stress in SCS-6/Ti-24Al-11Nb (Eldridge and Ebihara, 1994).

SCS-6 fiber and thus, acts as a weak interface between the fiber and the matrix. The low friction and wear at room temperature of graphite is attributed to water in the form of moisture, and secondarily oxygen adsorption (Savage, 1948). In the absence of adsorbed species (in vacuum), sliding graphite surfaces exhibited "dusting" wear, producing extremely fine debris. At room temperature in air, once the interface in SCS-6 fiber/matrix debonded, the gap created at the failed interface exposed both sides of the interface to the environment and the two surfaces could slide smoothly.

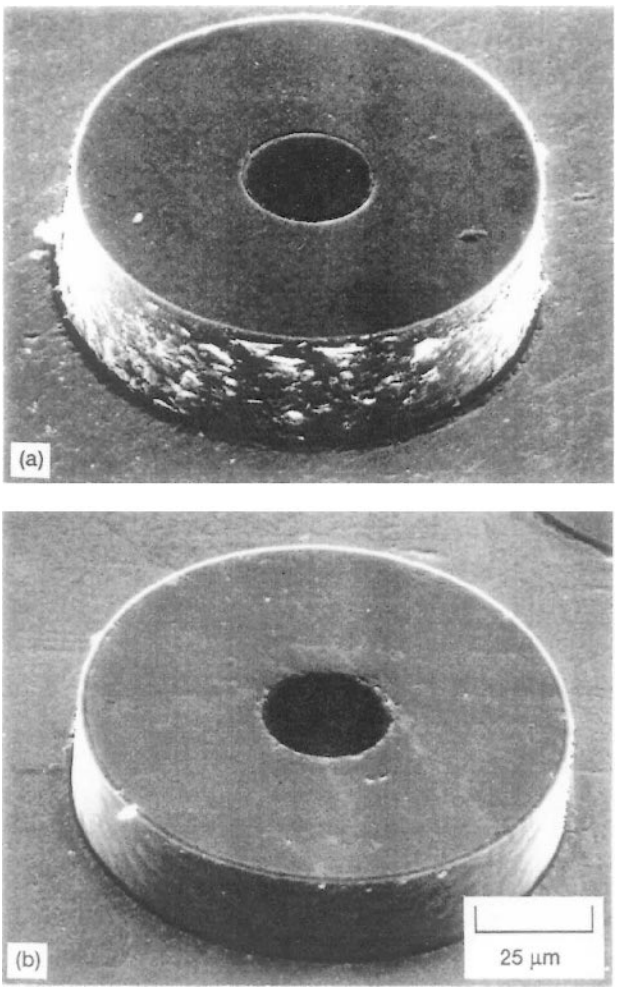

Fig. 5.8 SEM micrographs of pushed out fibers at (a) low temperature and (b) high temperature, showing a relatively rough and smooth surface, respectively (courtesy of J.I. Eldridge).

References

Arsenault, R.J., and R.M. Fisher, (1983) *Scripta Metall.*, **17**, 43.

Chawla, K.K., and Metzger, M., (1972) *J. Mater. Sci.*, **7**, 34.

Chawla, K.K. and M. Metzger, (1978) in *Advances in Research on Strength and Fracture of Materials*, Vol. 3, Pergaman Press, New York, p.1039.

Chawla, N., K.K. Chawla, M. Koopman, B. Patel, C. Coffin, and J.I. Eldridge, (2001) *Composites Sci. Tech.*, **61**, 1923.

Chawla, N., J.W. Holmes, and J.F. Mansfield, (1995) *Mater. Charac.*, **35** 199.

Cranmer, D.C., (1991) in *Ceramic and Metal Matrix Composites*, Pergamon Press, New York, p. 157.

Dlouhy, A., N. Merk, and G. Eggeler, (1993) *Acta Metall. Mater.*, **41**, 3245-3256.

Doerner, M.F., and W.D. Nix, (1986) *J. Mater. Res.*, **1**, 601.

Eldridge, J.I., and P.K. Brindley, (1989) *J. Mater. Sci. Lett.*, **8**, 1451.

Eldridge, J.I., and B.T. Ebihara, (1994) *J. Mater. Res.*, **9**, 1035.

Ferber, M.K., A.A. Wereszczsak, L. Riester, R.A. Lowden, and K.K. Chawla, (1993) *Ceram. Eng. Sci. Proc.*, **13**, 168.

Gabryel, C.M., and A.D. McLeod, (1991) *Metall. Trans*, **23A**, 1279.

Hill, R.G, R.P. Nelson, and C.L. Hellerich, (October, 1969) in *Proc. of the 16th Refractory Working Group Meeting*, Seattle, WA.

Kerans, R.J., and T.A. Parthasarathy, (1991) *J. Amer. Ceram. Soc.*, **74**, 1585.

Lancaster, J.K., and J.R. Pritchard, (1981) *J. Phys. D: Appl. Phys.*, **14** 747.

Liaw, P.K., Y. Ijiri, B.J. Taszarek, S. Frohlich, M.N. Gungor, and W.A. Logsdon, (1990) *Metall. Mater. Trans.*, **21**, 529-538.

Mandell, J.F., D.H. Grande, T.H. Tsiang, and F.J. McGarry, (1986) in *Composite Materials:Testing & Design*, ASTM STP 327, ASTM, Philadelphia, p. 87.

Mandell, J.F., K.C.C. Hong, and D.H. Grande, (1987) *Ceram. Eng. Sci. Proc.*, **8**, 937.

Marshall, D.B., (1984) *J. Amer. Ceram. Soc.*, **67**, C259.

Marshall, D.B., and W.C. Oliver, (1987) *J. Amer. Ceram. Soc.*, **70**, 542.

Marshall, D.B., M.C. Shaw, and W.L. Morris, (1992) *Acta Metall.*, **40**, 443.

Penn, L.S., and S.M. Lee, (1989) *J. Comp. Tech. & Res.*, **11**, 23.

Pfeifer, M., J.M. Rigsbee, and K.K. Chawla, (1990) *J. Mater. Sci.*, **25,** 1563.

Savage, R.H., (1948) *J. Appl. Phys.*, **19** 1.

Weihs, T.P., and W.D. Nix, (1991) *J. Amer. Ceram. Soc.*, **74**, 524.